Hierarchical Model Predictive Control for Coordinated Electric Railway Traction System Energy Management

Hrvoje Novak, *Student Member, IEEE,* Vinko Lešić, *Senior Member, IEEE,* and Mario Vašak, *Member, IEEE*

***Abstract*—The paper presents a railway energy management system based on hierarchical coordination of electric traction substation energy flows and on-route trains energy consumption. The railway system is divided into energy-efficient individual trains energy consumption management as lower level, and the price-efficient electric traction substation energy flows management as higher level. The levels are coordinated through parametric hierarchical model predictive control with the main goal of additionally increasing the energy efficiency and decreasing the operational costs of the overall system. Through interactions with the power grid on the higher level, the system is able to provide ancillary services and respond to various grid requests. At the same time, lower level trains driving profiles are adjusted to attain the minimal cost of system operation with timetables and on-route constraints respected. The developed algorithm is verified on a detailed real case study scenario put together with a railway operator and a trains manufacturer. The presented results show significant cost and energy consumption reductions achieved by simultaneous coordination of several trains supplied from the same traction substation.**

***Index Terms*—Train Traction Energy Consumption, Electric Traction Substation Energy Flows, Energy Management, Hierarchical Model Predictive Control.**

I. Introduction

In order to cope with the rise in transport demand and recent increase of railway activity [1], electric railway traction systems are a promising area for implementation of advanced energy management strategies with the goal of increasing energy efficiency and reduction of CO_2 emissions (emphasized in the European Union climate and energy targets for 2030 [2]). Besides the environmental benefits, the improvement in energy efficiency of the railway transport system increases economic profit and provides additional advantages for the railway infrastructure and train operators and the power system in general: (i) more efficient usage of the grid and smaller required grid capacity, (ii) increased power system reliability and stability through decentralization and (iii) reduction of required contracted power with significantly decreased operating costs. With integration of driver advisory systems, advanced energy meters, four-quadrant drives and various energy storage technologies, railway systems are transforming through smart control systems into active participants on the power grid.

Significant research focus of railway system energy efficiency is put on: (i) reducing the energy consumption of an individual train as in [3]–[11] and, more recently, on (ii) better utilization of regenerative braking energy, either by timetables optimization [12]–[14], or by introduction and implementation of different energy storage systems [15]–[21]. Energy-efficient train driving methods minimize energy consumption during train travel between adjacent stations while respecting the timetables, on-route restrictions (speed limits, train traction force boundaries etc.) and passengers comfort. Energy savings of up to 30% are reported in [22], where each train is considered individually without efficient exploitation of the regenerative energy produced by trains in braking. This is so far considered through optimization of timetables such that multiple trains acceleration and braking intervals are synchronized, which shows possible energy consumption reductions by up to 29%, with an extensive survey presented in [22]. Combination of multiple energy storage systems (batteries, supercapacitors and flywheels) introduces an additional energy savings potential of up to 30% [16]–[18]. However, train traction profiles are usually considered as constant and the possibility of their reshaping with respected timetable, route and comfort constraints is neglected. Therefore, the integrated approaches [23]–[26], that jointly optimize the timetable and trains driving profiles, are showing better performance since they take into account the minimization of the tractive energy consumption of each train while maximizing the utilization of regenerative energy between multiple trains. Listed railway system energy efficiency approaches exclude the power grid perspective. The focus is instead put solely on the processes and subsystems of the railway system. Possible benefits of railway system active interaction with the future electricity grids are presented in [27]–[32] showing the railway system ability to offer ancillary services to the power grid operator [27], integrate renewable energy sources [28]–[30], participate in the electricity market [31] and adapt to volatile electricity prices [32]. However, this is without consideration of timetables or train traction profiles optimization, thus disregarding the significant potential in their dynamic rearrangement.

In this paper, railway system is considered through

H. Novak, V. Lešić and M. Vašak are with Laboratory for Renewable Energy Systems (http://www.lares.fer.hr), University of Zagreb, Faculty of Electrical Engineering and Computing, Unska 3, HR-10000 Zagreb, Croatia (e-mail: hrvoje.novak@fer.hr, vinko.lesic@fer.hr, mario.vasak@fer.hr).

This work has been supported by Croatian Science Foundation under the project No. 6731 (project 3CON – Control-based Hierarchical Consolidation of Large Consumers for Integration in Smart Grids, http://www.fer.unizg.hr/3con), by the Danube Transnational Programme through the project Smart Building – Smart Grid – Smart City (3Smart, http://www.interreg-danube.eu/3smart), grant DTP1-502-3.2-3Smart, and by the European Regional Development Fund under the grant KK.01.1.1.01.0009 (DATACROSS).

coordination of on-route trains energy consumption and electric traction substation (ETS) energy flows management with the goal of increasing energy efficiency, decreasing operational costs and enabling integration of railways into smart electricity grids. The algorithm for hierarchical coordination is developed in several steps and described here together with an extensive case study scenario designed for verification of the developed control system within a realistic scenario taken from Croatian railways. The method for energy consumption minimization of a single train traveling between two stations was initially proposed in [33] where explicit constrained finite-time optimal control of piecewise affine systems is employed for calculation of the optimal traction force control law. On the higher, energy flows optimization level, model predictive control (MPC) problem is formulated with the linear cost function for the price-optimal energy flows, initially proposed in [32]. A single ETS is observed from the point of balancing energy flows between the accelerating and decelerating trains, the energy storage system and a connection to the utility grid with variable energy prices and various demands from the utility grid operator. Energy flows optimization results in optimal charging/discharging profiles for storage components that guarantee the optimal economic cost on the prediction horizon while taking into account the current state-of-charge of the energy storages, predicted trains consumption profile, volatile electricity price profile representing the economic criterion of the utility grid, and technical constraints on system components. The initial algorithm for coordination between the two levels is presented in [34] and is based on iterative improvement of the lower level solution through revisiting of both levels. Energy flows level model predictive control problem is locally solved parametrically with the lower level (optimal) energy consumption solution as a parameter. Lower level solution is then reoptimized with respect to higher level value function while taking into account the inherited lower level constraints. The developed algorithm is extended and validated on various simulation scenarios for different railway system operation set-ups with preliminary results presented in [35] showing the possibility for cost reductions of up to 25% for the specified scenario. The modularity and hierarchical structure of the presented algorithm keeps the considered subsystems operation apart since they are often required to remain infrastructurally and technologically independent, but also usually legally separated to infrastructure companies for operating power supply and different transportation companies for operating the trains. Due to the modular structure of the algorithm, the levels are able to operate independently when e.g. the train operation on the lower level cannot be changed. It is also possible to extend the proposed algorithm with new levels e.g. for simultaneous coordination of multiple traction substations such that a longer rail segment is considered.

The following contributions of the paper are highlighted: i) hierarchically coordinated multiple trains and ETS operation based on multi-parametric MPC approach verified on a detailed realistic simulation scenario, ii) modular energy management system adaptable to various railway system configurations simulated for one supply section of the railway, iii) simultaneous optimization of multiple trains traction profiles and utilization of regenerative braking energy based on real train parameters and timetables, and (iv) interaction of the ETS with the smart electricity grid through optimization of the operation costs with volatile electricity prices.

The paper is organized as follows. Problem definition and mathematical description of the control problems on both levels are presented in Section II. The concept of hierarchical coordination between the levels is elaborated in Section III. The realistic case study scenario is described in detail in Section IV together with the corresponding results presented in Section V. Finally, conclusions are given in Section VI.

II. Problem definition

Optimization problems for both on-route trains energy consumption (lower) and ETS energy flows management (higher) levels are described in the sequel. Superscripts 'l' and 'h' denote lower hierarchical level (LHL) and higher hierarchical level (HHL) variables, respectively. Lower and uppercase letters are used to denote vectors and matrices, respectively, while bold notation is used to denote variables stacked over the prediction horizon. Both problems are individually presented in [33] (LHL) and [32], [34] (HHL), and are for convenience presented in the sequel.

A. Lower hierarchical level

Train motion along the rail tracks is described with a simple continuous-time model [33]:

$$m\frac{\mathrm{d}v}{\mathrm{d}t} = F_{\mathrm{tr}} - F_{\mathrm{r}}(v,s), \quad \frac{\mathrm{d}s}{\mathrm{d}t} = v, \tag{1}$$

where m is the train mass, v the train velocity, F_{tr} the train traction force (in breaking $F_{\mathrm{tr}} < 0$), F_{r} the overall resistance force and s the traversed path. The resistance force F_{r} includes roll resistance (friction), aerodynamic resistance and track resistance (caused by track grade, curves and tunnels) and is nonlinear due to quadratic speed dependency and variable rail configuration:

$$F_{\mathrm{r}}(v,s) = \alpha_0(s) + \alpha_1 v + \alpha_2 v^2, \tag{2}$$

where α_0, α_1 and α_2 are resistance coefficients derived from the train shape, power train and other parameters.

Due to the non-linearity from (2) and model discretization effects, the train dynamics is described with a discrete-time piecewise affine (PWA) model:

$$\begin{aligned} x_{k+1} &= A_{\mathrm{d}i}x_k + B_{\mathrm{d}i}u_k + \gamma_{\mathrm{d}i}, \\ \text{if} \quad & H_i x_k + L_i u_k \leq K_i, \quad i = 1,2,3,4, \end{aligned} \tag{3}$$

where $x = \begin{bmatrix} v \\ s \end{bmatrix}$, $u = F_{\mathrm{tr}}$, matrices $A_{\mathrm{d}i}$, $B_{\mathrm{d}i}$ and $\gamma_{\mathrm{d}i}$ are obtained by Zero-Order Hold discretization of the continuous-time PWA model $\dot{x} = A_i x + B_i u + \gamma_i$ with sampling time T, $A_i = \begin{bmatrix} -\frac{a_i}{m} & 0 \\ 1 & 0 \end{bmatrix}$, $B_i = \begin{bmatrix} \frac{1}{m} \\ 0 \end{bmatrix}$, $\gamma_i = \begin{bmatrix} -\frac{b_i}{m} \\ 0 \end{bmatrix}$, coefficients a_i and b_i are obtained from linearization of the nonlinear resistance force from (2), and matrices H_i, L_i

and K_i are formed according to constraints for each PWA dynamics. Details on how the PWA model is obtained can be found in [33] with an extension towards a more detailed model presented in [36] where various traction and braking force limitations are included as well as a varying rail path configuration including slopes, curves and tunnels.

Mechanical energy required for the train within one sampling interval $I = \big[kT,(k+1)T\big)$ under constant $F_{\rm tr}(kT)$ applied along the entire interval I is:

$$\begin{aligned} E_I(F_{\rm tr}(kT),v(kT)) &= \textstyle\int_{kT}^{(k+1)T} F_{\rm tr}(kT)v(kT)dkT = \\ &= p_i(F_{\rm tr}(kT))^2 + q_iF_{\rm tr}(kT) + r_iF_{\rm tr}(kT)v(kT), \end{aligned} \tag{4}$$

where $T_i = \frac{m}{a_i}$, $p_i = \frac{1}{a_i}\left[T - T_i\left(1-e^{-\frac{T}{T_i}}\right)\right]$, $q_i = -b_ip_i$, $r_i = T_i\left(1-e^{-\frac{T}{T_i}}\right)$, the index i represents the currently activated dynamics. It is important to mention that $p_i > 0$ if $a_i > 0$, which leads to convex energy optimization problems with respect to the traction force [33].

Optimization of trains on-route energy consumption is formed as a minimization of trains energy cost during the travel time T^* dictated by the timetable:

$$\begin{aligned} J^{\rm l*} :=& \min_{\mathbf{u}^{\rm l},\mathbf{i}} \sum_{k=0}^{k^*} E_I(u_k^{\rm l}, x_k^{\rm l}), \\ &\text{s.t.} \begin{cases} x_{k+1}^{\rm l} = A_{{\rm d}i_k}x_k^{\rm l} + B_{{\rm d}i_k}u_k^{\rm l} + \gamma_{{\rm d}i_k}, \\ H_{i_k}x_k^{\rm l} + L_{i_k}u_k^{\rm l} \le K_{i_k}, \\ G^{\rm l}\begin{bmatrix} x_k^{\rm l} \\ u_k^{\rm l} \end{bmatrix} \le w^{\rm l}, \\ {\rm x}_{k^*}^{\rm l} = \begin{bmatrix} 0 \\ s_{k^*} \end{bmatrix}, \end{cases} \end{aligned} \tag{5}$$

where $u^{\rm l} = F_{\rm tr}$ is the train traction force, $x^{\rm l} = \begin{bmatrix} v \\ s \end{bmatrix}$ are the train states, i.e. train speed and traversed path, $k^* = T^*/T$, $i = 1,2,3,4$ mark the corresponding PWA train dynamics, E_I is described in (4), train dynamics are described with $A_{{\rm d}i}$, $B_{{\rm d}i}$ and $\gamma_{{\rm d}i}$, with corresponding dynamics constraints in H_i, K_i and L_i, maximal allowable and possible train traction force $F_{\rm tr,max}$ and speed $v_{\rm max}$ are described with $G^{\rm l}$ and $w^{\rm l}$, and s_{k^*} is the train position at the end of the route. Control problem formulated in (5) is a mixed-integer quadratic program and is solved backwards in time with dynamic programming through k^* steps. Detailed description of how the on-route train energy consumption optimization problem is formulated and solved can be found in [33] and [36]. The sampling time $T = 15$ seconds is chosen as a good trade-off between model precision and number of prediction instants on the prediction horizon of the LHL for the considered scenario.

The optimization problem on the LHL is composed of energy consumption minimization problems of all $j = 1,...,N_{\rm tr}$ trains currently supplied from the considered ETS. It is initially solved for all $N_{\rm tr}$ trains individually, while taking into account the train and rail path limitations together with preset timetables. The LHL problem results in energy-optimal traction/braking force sequences $\mathbf{u}_j^{\rm l*}$ and train speed and traversed path $\mathbf{x}_j^{\rm l*}$, together with fixed PWA dynamics switching sequences $\mathbf{i}_j^*$ for all trains:

$$\mathbf{u}_j^{\rm l*} = [u_{j,0}^{\rm l*},...,u_{j,k^*}^{\rm l*}], \tag{6}$$

$$\mathbf{x}_j^{\rm l*} = [x_{j,0}^{\rm l*},...,x_{j,k^*}^{\rm l*}]. \tag{7}$$

Optimal train traction sequence $\mathbf{u}_j^{\rm l*}$ and speed profile is plugged in (4), resulting in energy cost for a single train $\mathbf{E}_j^{\rm l*}$:

$$\mathbf{E}_j^{\rm l*} = [E_{j,0}^{\rm l*},...,E_{j,k^*}^{\rm l*}]. \tag{8}$$

Energy costs of all $N_{\rm tr}$ trains are summed to obtain the total ETS energy consumption, which is passed to the HHL level as a parameter $\boldsymbol{\theta}^{\rm h}$:

$$\boldsymbol{\theta}^{\rm h} = \sum_{j=1}^{N_{\rm tr}} \mathbf{E}_j^{\rm l*}. \tag{9}$$

In order to include the LHL problem from (5) in the hierarchical coordination algorithm, trains mechanical energy E_I from (4) needs to be linearized with respect to the train traction force $F_{\rm tr}$. Adaptation of the LHL problem to enable tuning of the traction profiles via hierarchical coordination is described in Section III.

B. Higher hierarchical level

Electric traction substation energy flows are consisted of accelerating trains energy consumption, decelerating trains energy production, wayside energy storage system energy flows and energy exchanged with the electrical grid. The power balance of the system is:

$$P^{\rm TR} = P^{\rm G} + P^{\rm SC} + P^{\rm BAT} + P^{\rm R}, \tag{10}$$

where $P^{\rm TR}$ denotes the cumulative power consumption ($P^{\rm TR} > 0$) or production ($P^{\rm TR} < 0$) by trains supplied from the ETS, $P^{\rm G}$ denotes the power exchanged with the electrical power grid, $P^{\rm SC}$ and $P^{\rm BAT}$ denote supercapacitor and battery power flows, respectively, and $P^{\rm R}$ is the power dissipated on the ETS resistors.

The considered energy storage systems are modeled with:

$$\begin{aligned} x_{k+1}^{\rm BAT} &= x_k^{\rm BAT} - \frac{T}{C^{\rm BAT}}\left(\frac{1}{\eta_{\rm dch}^{\rm BAT}}P_{{\rm dch},k}^{\rm BAT} + \eta_{\rm ch}^{\rm BAT}P_{{\rm ch},k}^{\rm BAT}\right), \\ x_{k+1}^{\rm SC} &= x_k^{\rm SC} - \frac{T}{C^{\rm SC}}\left(\frac{1}{\eta_{\rm dch}^{\rm SC}}P_{{\rm dch},k}^{\rm SC} + \eta_{\rm ch}^{\rm SC}P_{{\rm ch},k}^{\rm SC}\right), \end{aligned} \tag{11}$$

where states $x_k^{\rm BAT}$ and $x_k^{\rm SC}$ are normalized battery and the supercapacitor state-of-charge (SoC), respectively, C is storage capacity, $\eta_{\rm ch}$ and $P_{\rm ch}$ are charging efficiency and charging power component of the storage system ($P_{\rm ch} \le 0$), while $\eta_{\rm dch}$ and $P_{\rm dch}$ are discharging efficiency and discharging power component of the storage system ($P_{\rm dch} \ge 0$). Separation of charging and discharging is introduced to avoid additional integer formulation [37].

Traction substation microgrid energy flows optimization is formulated as a model predictive control (MPC) HHL problem

with the cost function set as the economic criterion of overall system operation on the prediction horizon N:

$$J^{\mathrm{h}*} := \min_{P^{\mathrm{BAT}}_{\mathrm{ch,dch},k}, P^{\mathrm{SC}}_{\mathrm{ch,dch},k}, P^{\mathrm{R}}_{k}} T \sum_{k=0}^{N-1} c_k P^{\mathrm{G}}_{k}, \tag{12}$$

where $\mathbf{c}$ denotes the utility electricity price in €/MWh.

The MPC problem, as reported in [32], takes into account the ETS physical constraints, energy storage SoC and charging/discharging power limitations and limitations on energy exchanged with the grid. Microgrid physical constraints are introduced to the control problem as state and input constraints. With respect to energy storage system dynamics from (11), constraints include supercapacitor and battery SoC limitations in order to preserve the health of the storage systems:

$$\begin{aligned} x^{\mathrm{SC}}_{\min} \leq x^{\mathrm{SC}}_{k} \leq x^{\mathrm{SC}}_{\max}, \\ x^{\mathrm{BAT}}_{\min} \leq x^{\mathrm{BAT}}_{k} \leq x^{\mathrm{BAT}}_{\max}, \end{aligned} \tag{13}$$

and maximum charging and discharging power of the supercapacitor and batteries:

$$\begin{aligned} P^{\mathrm{BAT}}_{\mathrm{dch,min}} \leq P^{\mathrm{BAT}}_{\mathrm{dch},k} \leq P^{\mathrm{BAT}}_{\mathrm{dch,max}}, \\ P^{\mathrm{BAT}}_{\mathrm{ch,min}} \leq P^{\mathrm{BAT}}_{\mathrm{ch},k} \leq P^{\mathrm{BAT}}_{\mathrm{ch,max}}, \\ P^{\mathrm{SC}}_{\mathrm{dch,min}} \leq P^{\mathrm{SC}}_{\mathrm{dch},k} \leq P^{\mathrm{SC}}_{\mathrm{dch,max}}, \\ P^{\mathrm{SC}}_{\mathrm{ch,min}} \leq P^{\mathrm{SC}}_{\mathrm{ch},k} \leq P^{\mathrm{SC}}_{\mathrm{ch,max}}. \end{aligned} \tag{14}$$

Constraints on utility grid power rating are defined as follows:

$$P^{\mathrm{G}}_{\min} \leq P^{\mathrm{G}}_{k} \leq P^{\mathrm{G}}_{\max}, \tag{15}$$

and constraints on the power dissipated in the resistors as:

$$0 \leq P^{\mathrm{R}}_{k} \leq P^{\mathrm{R}}_{\max}. \tag{16}$$

For simplification, excess regenerative energy is dissipated on the virtual resistors bank, while it is actually substituted with the use of frictional brakes instead of regenerative braking proportionally distributed over all trains in braking. Due to the MPC philosophy, the system takes into account future electricity prices c, available one day in advance, as well as the predicted energy consumption/production of all trains currently supplied from the ETS and is therefore able to plan the future consumption in advance such that the system acts as a flexible and proactive consumer connected to the grid.

The HHL optimization problem minimizes the cost of energy exchanged between the ETS that supplies the considered rail section and the transmission power grid. The HHL problem introduced in (12) is reformulated as a multi-parametric MPC optimization problem with the parameters set $\boldsymbol{\theta}^{\mathrm{h}}$ obtained from the LHL solution (9):

$$\begin{aligned} J^{\mathrm{h}*} := & \min_{\mathbf{u}^{\mathrm{h}}} \mathbf{h}^{\mathrm{h}} \begin{bmatrix} \mathbf{x}^{\mathrm{h}} \\ \mathbf{u}^{\mathrm{h}} \end{bmatrix} + \mathbf{f}^{\mathrm{h}} \boldsymbol{\theta}^{\mathrm{h}}, \\ & \text{s.t.} \begin{cases} \mathbf{x}^{\mathrm{h}} = \mathbf{A}^{\mathrm{h}} x^{\mathrm{h}}_{0} + \mathbf{B}^{\mathrm{h}} \mathbf{u}^{\mathrm{h}}, \\ \mathbf{G}^{\mathrm{h}} \begin{bmatrix} \mathbf{x}^{\mathrm{h}} \\ \mathbf{u}^{\mathrm{h}} \end{bmatrix} \leq \mathbf{w}^{\mathrm{h}} + \mathbf{E}^{\mathrm{h}} \boldsymbol{\theta}^{\mathrm{h}}, \end{cases} \end{aligned} \tag{17}$$

where $\mathbf{h}^{\mathrm{h}}$ and $\mathbf{f}^{\mathrm{h}}$ are computed from (12) and represent the cost of the energy exchanged with the transmission grid, $\mathbf{x}^{\mathrm{h}}$ is the storages SoC with $\mathbf{A}^{\mathrm{h}}$ and $\mathbf{B}^{\mathrm{h}}$ representing the dynamics of the storage systems from (11), $\mathbf{u}^{\mathrm{h}} = \left[\boldsymbol{P}^{\mathrm{BAT}}_{\mathrm{ch}}, \boldsymbol{P}^{\mathrm{BAT}}_{\mathrm{dch}}, \boldsymbol{P}^{\mathrm{SC}}_{\mathrm{ch}}, \boldsymbol{P}^{\mathrm{SC}}_{\mathrm{dch}}, \boldsymbol{P}^{\mathrm{R}}\right]$ incorporates charging/discharging energies of the energy storage system and dissipating on the resistor bank, while $\mathbf{G}^{\mathrm{h}}$, $\mathbf{w}^{\mathrm{h}}$ and $\mathbf{E}^{\mathrm{h}}$ are used to describe the HHL physical constraints and limitations presented in (13)-(16).

III. Hierarchical coordination for energy management

Hierarchical coordination between the LHL and HHL is performed through revisiting of both control levels with the goal of improving the initial energy-optimal LHL solution for individual trains with respect to the HHL cost for energy exchange, thus transforming it into a global, price-optimal, solution for all trains. The iterative coordination scheme is depicted in Fig. 1, executed until the LHL solution converges with respect to the global criteria under the given constraints, i.e. when the train traction force energy-optimal profile is shifted to the price-optimal profile.

Local multi-parametric HHL problem from (17) is solved for the initial LHL solution $\boldsymbol{\theta}^{\mathrm{h}}$ as a parameter. In the case of an infeasible HHL optimization problem (17) with initially obtained $\boldsymbol{\theta}^{\mathrm{h}}$, the nearest feasible $\boldsymbol{\theta}^{\mathrm{h}}$ is calculated and introduced into the HHL. By applying the geometric multi-parametric algorithm from [38], only a single critical region (CR) is computed around the LHL solution and no additional partitioning of the parameter space is performed. A critical region is a subset of parameters $\boldsymbol{\theta}^{\mathrm{h}}$ that yield the same set of active constraints, i.e. constraints that are satisfied with equality in the optimal solution. For the computed LHL solution, CR boundaries around it are defined as:

$$\mathbf{G}^{\mathrm{h,CR}} \boldsymbol{\theta}^{\mathrm{h}} \leq \mathbf{w}^{\mathrm{h,CR}}, \tag{18}$$

while the optimal control law and value function characterization are linear over the CR, i.e. for any cumulative trains consumption profiles within the CR, are formulated as:

$$\mathbf{u}^{\mathrm{h}*}(\boldsymbol{\theta}^{\mathrm{h}}) = \mathbf{D}^{\mathrm{h,CR}} \boldsymbol{\theta}^{\mathrm{h}} + \mathbf{Q}^{\mathrm{h,CR}}, \tag{19}$$

$$J^{\mathrm{h,CR}*}(\boldsymbol{\theta}^{\mathrm{h}}) = \mathbf{h}^{\mathrm{h,CR}} \boldsymbol{\theta}^{\mathrm{h}} + \mathbf{f}^{\mathrm{h,CR}}. \tag{20}$$

The calculated CR boundaries and value function are then passed to the LHL in order to reoptimize the previously obtained train traction sequences. Since HHL is set on minimization of the cost for energy exchanged with the power grid, CR boundaries $\mathbf{G}^{\mathrm{h,CR}}$, $\mathbf{w}^{\mathrm{h,CR}}$ and value function $\mathbf{h}^{\mathrm{h,CR}}$, $\mathbf{f}^{\mathrm{h,CR}}$ are functions of trains energy and need to be transformed in order to adapt them to LHL traction force based optimization (5). Otherwise, the optimization problem on the LHL becomes nonlinear since the trains consumed energy (4) is a quadratic function of the traction force which would be introduced in CR constraints (18), thus making the LHL problem non-convex and hard to solve in real-time applications. The linearization is performed around the current solution of the traction force sequence from LHL (6). Although the CR value function from (20) could be kept

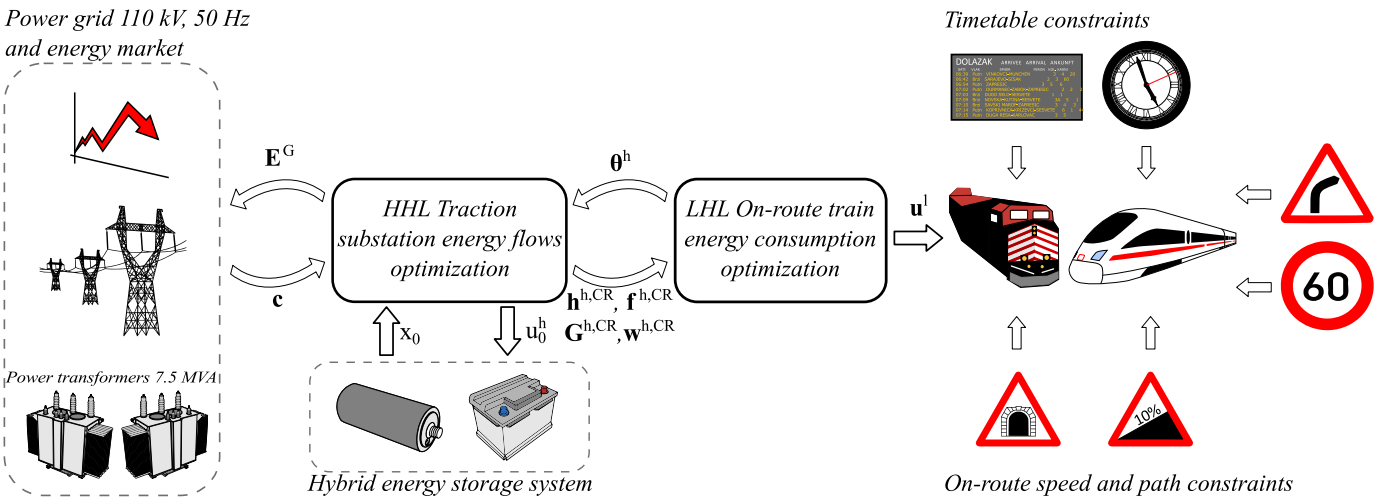

Fig. 1: Scheme and information flow of hierarchical coordination between LHL and HHL optimizations.

quadratic with respect to the traction forces $\mathbf{u}^{\mathrm{l}}$, it is linearized since linear programs are easier to solve and have better solving properties in terms of speed and convergence. After linearization, LHL is optimized with respect to the CR value function and CR boundaries for all N_{tr} simultaneously, while taking into account LHL constraints of all N_{tr} trains currently supplied from the ETS. The reformulated LHL optimization problem is solved for all N_{tr} trains while keeping the new solution in close vicinity of the initial LHL solution in order to ensure the linearization accuracy:

$$
\begin{aligned}
J^{\mathrm{h,CR}*} := \min_{\Delta \mathbf{u}^{\mathrm{l}}} \; & \mathbf{h}_{\mathrm{lin}}^{\mathrm{h,CR}}(\mathbf{u}^{\mathrm{l}} + \Delta \mathbf{u}^{\mathrm{l}}) + \mathbf{f}_{\mathrm{lin}}^{\mathrm{h,CR}}, \\
\text{s.t.} \; & \begin{cases}
-\boldsymbol{\varepsilon} \leq \Delta \mathbf{u}^{\mathrm{l}} \leq \boldsymbol{\varepsilon}, \\
\mathbf{G}_{\mathrm{lin}}^{\mathrm{h,CR}}(\mathbf{u}^{\mathrm{l}} + \Delta \mathbf{u}^{\mathrm{l}}) \leq \mathbf{w}_{\mathrm{lin}}^{\mathrm{h,CR}}, \\
\mathbf{G}_j^{\mathrm{l}} \begin{bmatrix} \mathbf{x}_j^{\mathrm{l}} \\ (\mathbf{u}_j^{\mathrm{l}} + \Delta \mathbf{u}_j^{\mathrm{l}}) \end{bmatrix} \leq \mathbf{w}_j^{\mathrm{l}}, \\
\quad \vdots \\
\mathbf{G}_{N_{\mathrm{tr}}}^{\mathrm{l}} \begin{bmatrix} \mathbf{x}_{N_{\mathrm{tr}}}^{\mathrm{l}} \\ (\mathbf{u}_{N_{\mathrm{tr}}}^{\mathrm{l}} + \Delta \mathbf{u}_{N_{\mathrm{tr}}}^{\mathrm{l}}) \end{bmatrix} \leq \mathbf{w}_{N_{\mathrm{tr}}}^{\mathrm{l}},
\end{cases}
\end{aligned}
\tag{21}
$$

where $\mathbf{u}^{\mathrm{l}} = [\mathbf{u}_j^{\mathrm{l}}, \cdots, \mathbf{u}_{N_{\mathrm{tr}}}^{\mathrm{l}}]$, $\Delta \mathbf{u}^{\mathrm{l}}$ is the change with respect to the initial LHL solution $\mathbf{u}^{\mathrm{l}}$, $\boldsymbol{\varepsilon}$ is the change limitation added to insure the linearization accuracy, $\mathbf{h}_{\mathrm{lin}}^{\mathrm{h,CR}}$ and $\mathbf{f}_{\mathrm{lin}}^{\mathrm{h,CR}}$ are the linearized coefficients of the CR value function from (20), $\mathbf{G}_{\mathrm{lin}}^{\mathrm{h,CR}}$ and $\mathbf{w}_{\mathrm{lin}}^{\mathrm{h,CR}}$ are the linearized CR boundaries and $\mathbf{G}_j^{\mathrm{l}}$ and $\mathbf{w}_j^{\mathrm{l}}$ are LHL constraints of train j from (5) with included PWA train dynamics sequence constraints and end-state constraints ensuring punctual arrival at the station. In the reformulated LHL optimization problem (21), the initial LHL cost function J^{l} from (5), for an individual train, is substituted with the CR value function from (20) representing the minimum cost for energy consumption of all the trains simultaneously, with respect to the change of the initial LHL solution $\Delta \mathbf{u}^{\mathrm{l}}$.

As presented in Fig. 1, the subproblems interact through exchange of several variables. The LHL subproblem from (21) generates optimal traction profiles for all the trains supplied from a single ETS and sends the overall trains energy consumption profile $\boldsymbol{\theta}^{\mathrm{h}}$ to the HHL subproblem where it is used as an optimization parameter. The HHL then calculates a single critical region with the corresponding value function parameters $\mathbf{h}^{\mathrm{h,CR}}$, $\mathbf{f}^{\mathrm{h,CR}}$ and critical region boundaries $\mathbf{G}^{\mathrm{h,CR}}$, $\mathbf{w}^{\mathrm{h,CR}}$ and passes them to the LHL where the trains traction profiles are reoptimized and tuned according to the critical region value function from (21). New traction profiles are created in the LHL and returned to the HHL. There are several different possibilities of how the hierarchical coordination is continued with respect to the constraints activated at the optimal solution of (21):

- linearization accuracy constraints are activated; linearization is then performed around the new force sequence and LHL is solved again,
- CR boundaries are reached; the solution is transfered to the adjacent CR on the HHL which requires to solve (17) and characterize the new CR, and (21) is then solved again,
- dynamics switching sequence constraints of the trains LHL PWA model, found within constraints described with $\mathbf{G}_j^{\mathrm{l}}$, $\mathbf{w}_j^{\mathrm{l}}$ for train j, are activated for some of the trains, new dynamics switching sequences are found through solving a mixed-integer linear program described in [35] and (21) is then solved again with these new switching sequences introduced in corresponding constrains formed by $\mathbf{G}_j^{\mathrm{l}}$, $\mathbf{w}_j^{\mathrm{l}}$.

When all options are exhausted and LHL solution converges, i.e. $\|\Delta \mathbf{u}^{l}\| \leq \xi$, where ξ is the allowed tolerance, the procedure is concluded. The flowchart of the overall algorithm, including also the details of hierarchical coordination, is depicted in Fig. 2.

Through the described coordination, the trains maintain the schedule in timetables, and respect their physical constraints and route limitations. At the same time they are coordinated with the ETS optimal energy flows through prices $\mathbf{h}_{\mathrm{lin}}^{\mathrm{h,CR}}$ and $\mathbf{f}_{\mathrm{lin}}^{\mathrm{h,CR}}$. This way, the energy is distributed among all the trains that are currently supplied from a single ETS and the overall price-optimal system operation is achieved. The

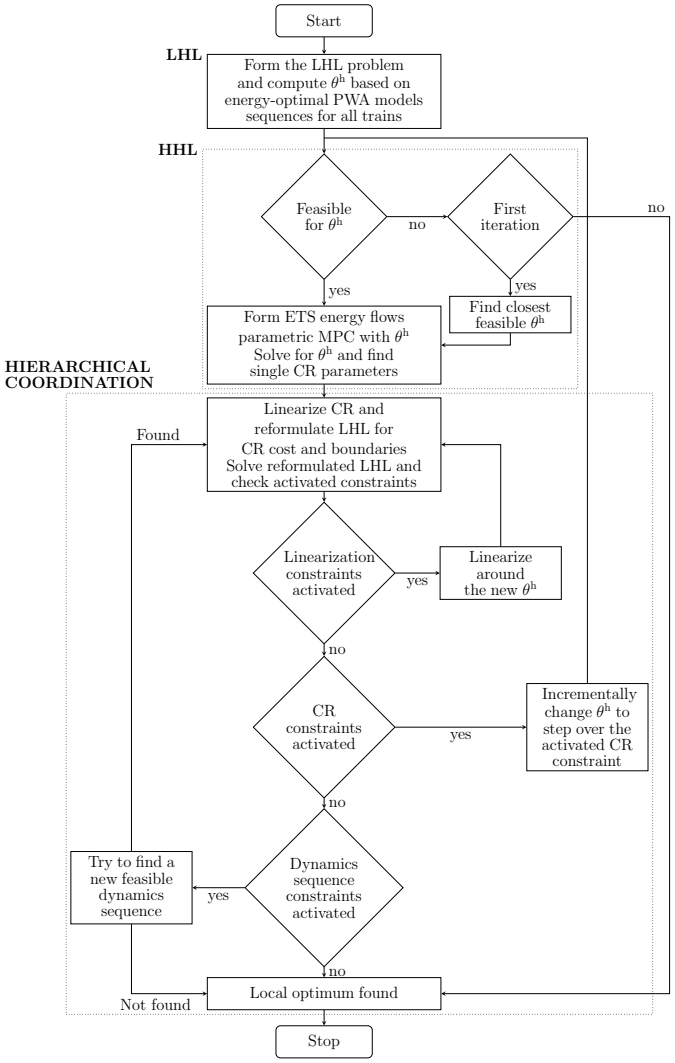

Fig. 2: Hierarchical coordination algorithm flow chart.

railway system is thus transformed from a passive energy consumer into a proactive flexible participant connected to the power grid, which is then able to provide ancillary services (e.g. secondary services such as frequency regulation) to the power grid as well as actively respond to power grid demands (e.g. temporary consumption reduction/increase, power peak shaving etc.).

IV. Case study simulation scenario

The validation environment and simulation models are put together such that a realistic system behavior is simulated for application of control algorithms developed in [32], [34] and [35]. The case study is based on actual trains, time schedules and rail route configurations. The trains time-schedule and rail route configuration are taken from the railway section of Corridor X of Croatian Railways Infrastructure which is supplied from ETS Andrijevci in Slavonia region (eastern Croatia) [39]. The train configuration considered belongs to the low-floor electromotive train (EMT) for urban and commuter operation manufactured by Končar – Electric Vehicles Inc. [40], [41]. The chosen simulation environment serves as a base case representative for many different railway systems. Railway segment comprised of straight rail tracks with no slopes or curves and electromotive trains with the ability of regenerative braking, all together supplied from the power grid through a single connection point in the ETS is one of the most commonly found railway system setups and is easily extended towards different, more complex setups. Different rail paths were studied on the lower hierarchical level with results published in [36] showing it is possible to extended the presented algorithm on more complex railway configurations including slopes, curves and tunnels.

A. Train composition model

The considered electromotive train is intended for urban and commuter operation and is designed as a low-floor four-part train with the total length of 75 m. It is built for rails electrified with catenary power supply of 25 kV voltage and 50 Hz frequency with maximum speed of 160 km/h.

Train braking system is designed as a combination of regenerative and pneumatic frictional brakes which together provide the necessary braking force. Pneumatic frictional braking is utilized in lower speeds when regenerative braking is not able to provide enough braking force to stop the train [40], [41]. Parameters of the Končar EMT are presented in Table I together with resistance and available traction/braking force curves in Fig 3. For optimal train traction control law computation a DTPWA train model is computed by implementing the procedure described in [36] where the resistance force F_{r} is linearized and conservative constraints for available traction and braking force F_{tr} are introduced to the DTPWA model (3).

TABLE I: Končar low-floor electromotive train parameters.

Parameter	Value
Catenary supply voltage	25 [kV], 50 [Hz]
Composition weight	139 [t]
Max. weight	172 [t]
Overall length	75 [m]
Gauge	1435 [mm]
Powered bogie axle/wheel radius	180/750 [mm]
Trailer bogie axle/wheel radius	180/860 [mm]
Continuous power (on wheel)	2000 [kW]
Starting traction force	200 [kN]
Max. acceleration at gross weight	1 [m/s^2]
Max. deceleration	1.3 [m/s^2]
Max. velocity	44.44 [m/s]
Specific resistance force	$856 + 36v + 5.4432v^2$ [N]
Motor-reductor efficiency	0.939
Converter efficiency	0.95

Optimal train traction force for the corresponding DTPWA model of Končar's EMT is calculated using the procedure proposed in [33], for different train travel times and distances.

B. Rail configuration

The considered ETS selected within the so-called Corridor X of the Croatian railway operator, which is entirely electrified, can withstand the maximum train velocity of 160 km/h and has double track gauges for simultaneous two-way traffic. A part of Corridor X supplied from ETS Andrijevci

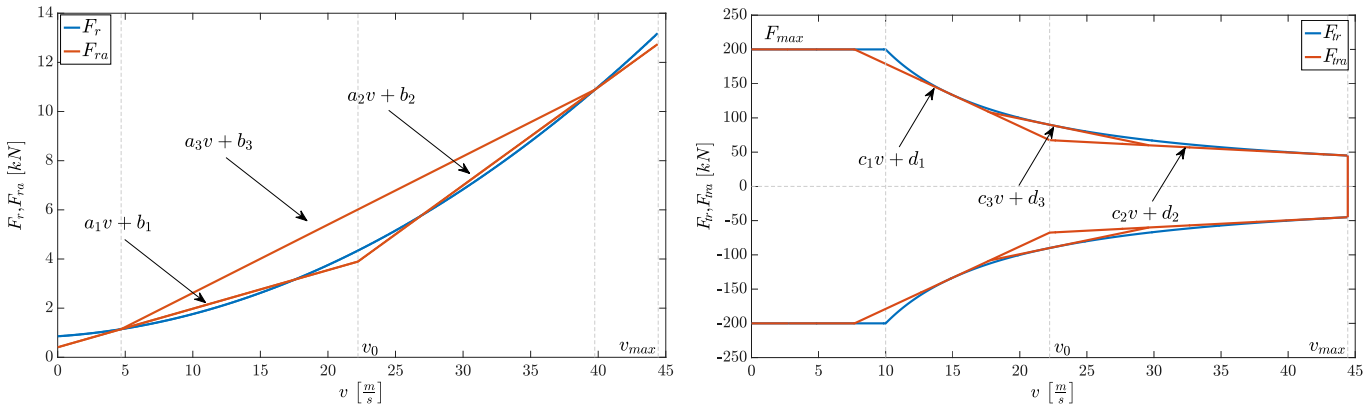

(a) Overall resistance force F_{r} to train movement.

(b) Available traction and braking force boundaries.

Fig. 3: Končar low-floor electromotive linearized train resistance F_{ra} and available traction force boundaries F_{tra} [36].

is selected with small to none track gradient and no curves or tunnels. Andrijevci ETS is situated between ETS Jankovci and ETS Nova Kapela. The area supplied by ETS Andrijevci covers track length between two facilities with neutral conduit sections (NS), namely NS Ivankovo and NS Sibinj. Following from distance between NS Ivankovo and NS Sibinj, it is assumed that ETS Andrijevci supplies a traction segment of ~ 56 km including 10 passenger stations. The considered rail path is depicted in Fig. 4.

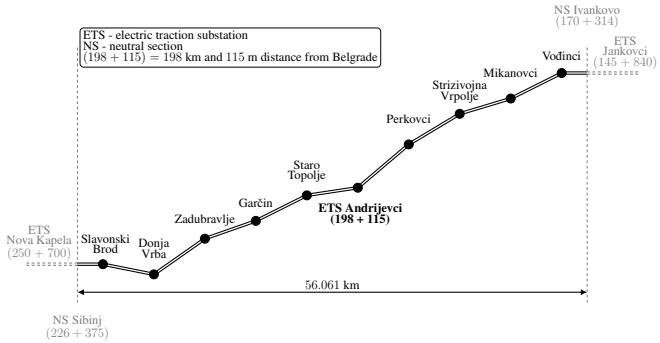

Fig. 4: Croatian Railways Corridor X section area supplied from ETS Andrijevci with the corresponding passenger stations.

The corresponding passenger stations locations with travel distances and times are presented in Table II. Traveling times between passenger stations have been obtained from the official railway timetable of Croatian Railways for the period from 14/12/2014 to 12/12/2015. Since different trains have different travel times, average travel times are used and presented in Table II. It is assumed that each train spends one minute in each passenger station in order to allow passengers to board and leave the train. When summed, the whole trip from Slobodnica station to Ivankovo station lasts 62 minutes and 30 seconds. It is important to notice that during the whole trip the train is supplied from ETS Andrijevci only between two neutral sections NS Sibinj and NS Ivankovo, therefore the route considered in the simulation lasts around one hour.

TABLE II: Passenger stations supplied from ETS Andrijevci.

Station (location in km+m from Belgrade)	Distance to next station [km]	Travel time to next station [min]
Slobodnica (227 + 468)	6.777	7
NS Sibinj (226 + 375)	–	–
Slavonski Brod (220 + 691)	8.755	6.5
Donja Vrba (211 + 936)	2.582	3
Zadubravlje (209 + 354)	2.611	3
Garčin (206 + 743)	4.920	4
Staro Topolje (201 + 823)	3.635	4
ETS Andrijevci (198 + 118)	4.869	3.5
Perkovci (193 + 249)	5.452	5
Strizivojna–Vrpolje (187 + 797)	10.846	7
Stari Mikanovci (176 + 951)	5.873	4.5
Vođinci (171 + 078)	4.329	4
NS Ivankovo (170 + 314)	–	–
Ivankovo (166 + 749)	10.885	7

C. ETS parameters

ETS validation environment is considered from a standpoint of energy flows between the trains consumption and regeneration, ETS with the corresponding energy storage system and the power grid with volatile energy prices. Renewable energy sources like photovoltaic panels or small scale wind turbines built in/on passengers stations are not considered because of a rather small power production contribution in comparison to the overall trains consumption in megawatt scale but can be easily introduced as disturbance in HHL optimization problem (17). Therefore the only considered power generation in the ETS is the regenerative braking energy produced by trains.

1) Utility grid connection: Connection to the utility grid is made via two $110/25$ kV transformers of 7.5 MVA power each. The ETS power rating of 15 MVA is the most commonly found case of ETS transformers in Croatian railways. The transformers have the ability to return energy back to the utility grid which offers a possibility for interaction with the power grid and better utilization of excessive regenerative and/or stored energy. However there are also constraints on the power grid side, limiting the amount of energy that can be returned back to the grid in order to ensure grid stability. The limit for energy returned into the grid is set to 1 MW.

In the case of excessive regenerative braking power that

cannot be delivered to the utility grid ($P_{\mathrm{R}} > 0$), the proposed control system distributes the amount of excessive energy among the trains supplied from the ETS that are in braking, proportionally to their braking energy. The regenerative braking on each train is then reduced to fit the available amount during one time instant while the remaining braking force is substituted with the use of frictional brakes and modeled with energy dissipated on the resistors. If the power consumption of the trains auxiliary systems is considered on the LHL, it is expected that the amount of excessive regenerative energy is reduced since the power consumption of all trains would increase, i.e. the regenerative braking power would decrease.

The current energy pricing scheme in Croatia is based on a two-tariff pricing for buying energy with higher prices set during the day and lower during the night, and with no reimbursement when selling energy, i.e. returning it to the grid. However, it is expected that price profiles varying on hourly or even smaller time-scales will be implemented in the near future. The considered prices for energy exchange are based on European Power Exchange prices (EPEX [42]), which are available one day ahead. For simplicity, prices for energy exchange with the grid do not change when buying or selling energy, while the case with no reimbursement for selling energy is simulated with the 0 MW limit on the energy returned to the grid.

2) Energy storage system: The considered energy storage system is modeled as a joint operation of battery energy storage system and a supercapacitor. The use of such storage systems has been discussed throughout the literature [17], [18], [27], [28] with commercially available technologies such as supercapacitors from Maxwell Technologies, Inc. [43] or Saft Batteries trackside battery storage systems [44]. Selection of the supercapacitor is justified for collecting the regenerative braking energy with large number of charging/discharging cycles, due to its large power density, while battery storage is selected with the aim of collecting larger amounts of energy during longer periods of time, due to the batteries high energy density. The considered energy storage system parameters are listed in Table III.

TABLE III: Energy storage system parameters.

Parameter	Battery storage	Supercapacitor
Rated power [MW]	0.3	1.2
Capacity [kWh]	140	30
Charge/Discharge efficiency	0.8	0.95
Maximum SoC	0.9	0.9
Minimum SoC	0.1	0.1
Initial SoC	0.1	0.1

V. Results

A. LHL control – individual train energy consumption

For the train model described with parameters in Table I energy-efficient traction profiles are calculated for a single travel between two stations as well as for the travel throughout the whole ETS Andrijevci supply area with the results presented as follows.

1) Single travel: the route between passenger stations Slobodnica and Sl. Brod is simulated with the resulting energy-optimal traction force profile presented together with speed and traversed path profiles in Fig 5. Stations are distanced 6.8 km with designated travel time of 7 minutes according to Croatian Railways timetable (Fig. 4 and Table II).

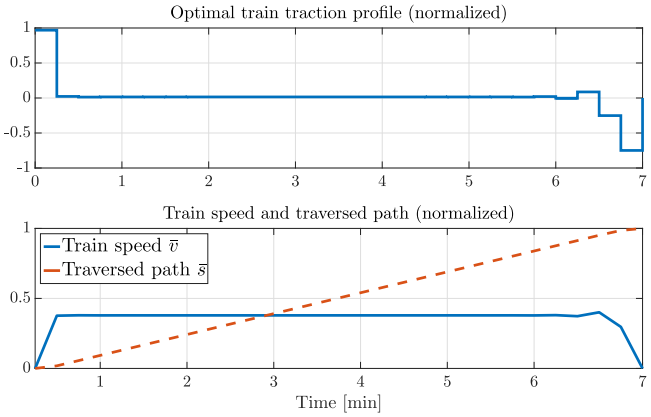

Fig. 5: Energy-optimal train traction force, speed and traversed path profiles while traveling from Slobodnica to Sl. Brod.

2) ETS Andrijevci supply area: traveling through ETS Andrijevci supply area lasts around 60 minutes (including 1 minute stops in all passenger stations) according to the Croatian railways timetable (as presented in Table II) for the rail path length of 60.7 km and travel time duration of 62 minutes and 30 seconds (including one-minute stops in passenger stations). The calculated energy-optimal train traction force profile is presented in Fig. 6 together with the corresponding travel speed and traversed path profiles. Figures 5 and 6 also show that it is economically more viable to maintain lower speed for most of the path and speed up at the end of the route to satisfy the time-schedule constraints, which is manifested as peaks in traction and speed in the opposite direction at the beginning and end of the cruising phase.

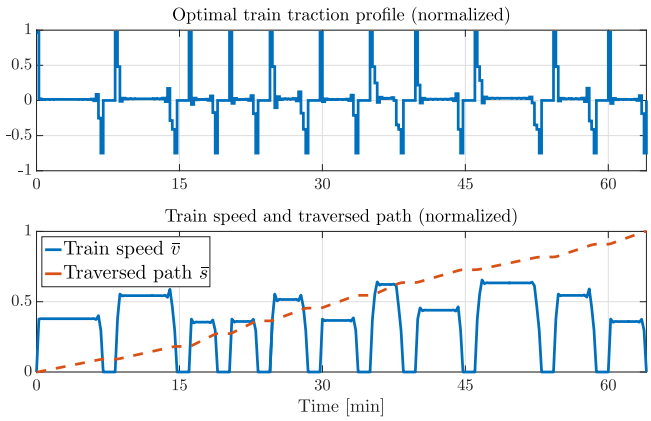

Fig. 6: Energy-optimal train traction force, speed and traversed path profiles while traveling from Slobodnica to Ivankovo.

Since there is no measured data available on the Končar EMV train energy consumption on the Slobodnica-Ivankovo route, the savings from implementation of the sole LHL

control system cannot be exactly calculated but are expected to be around 30% compared to average driver performance, according to comprehensive survey papers [5], [22].

B. HHL control – ETS power flows

After the initial results are obtained from the LHL, energy-optimal train travel consumption profile is created for a train traveling through the ETS Andrijevci supply area, as presented in Fig. 5. To simulate the Croatian railways timetable for the considered ETS Andrijevci area during one day, created travel profiles are stacked in time with all the passenger trains considered identical to the presented Končar EMT.

With the installation of energy storages (as presented in Subsection IV-C2) the higher MPC system is implemented and HHL control system operation is simulated during a daily system operation according to the Croatian railways timetable together with volatile EPEX prices and a prediction horizon of $N = 24$ h. Simulation scenario results are depicted in Fig. 7 and comprise of: (i) energy exchange price profile, (ii) ETS power flows (summed trains energy consumption/production), (iii) energy exchanged with the utility grid and (iv) energy storage state of charge for both energy storage components (battery system and supercapacitor).

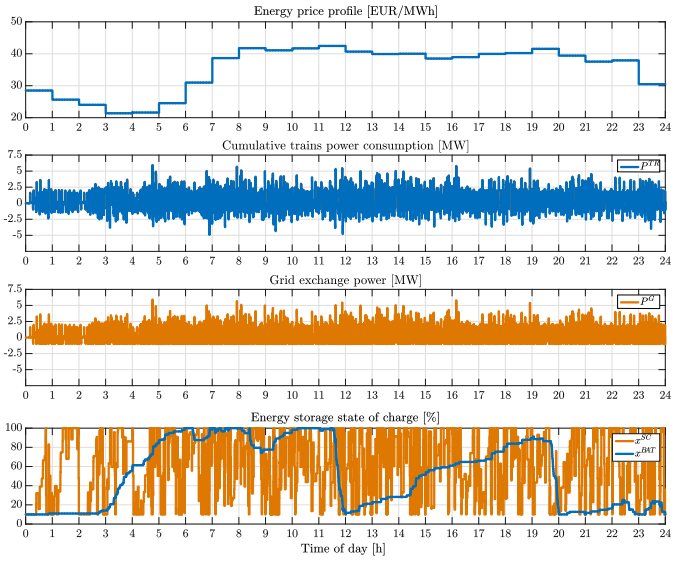

Fig. 7: Daily power flows for system operation with only higher level MPC installed and grid receptiveness of -1 MW.

System operation has been simulated for different grid receptiveness levels of 5, 3, 1 and 0 MW of power that can be returned to the grid. The system is also simulated for a fixed-price tariff (same energy exchange price throughout the day), two-prices tariff (cheaper energy exchange price during the night) and with the variable-price tariff as described in Section IV-C1. From the obtained cost savings results, presented in Fig. 8, it can be observed that the possible savings reach 35% on the HHL alone and rise when the grid is more conservative, meaning that little or no energy can be returned to the grid. For the case when grid receptiveness is set to 5 MW (or above), all of the regenerative braking energy can be returned to the grid due to the fact that a maximum of 7 trains is simultaneously supplied from the considered ETS and the regenerative braking power never exceeds 5 MW during one time instant. In such a scenario the algorithm has very little space to reduce the operation costs since there is no excess energy in the system. All that remains is the price variability, which is then exploited through charging and discharging of the energy storage system with little cost reductions (as shown in Fig. 8). Highest savings are obtained for the case when no energy can be returned to the grid (0 MW) meaning that all of the regenerative braking energy that is not immediately used by other trains or stored in the energy storage system is dissipated and lost. In such a scenario there is a significant possibility of storing the regenerative energy for later use which results in cost reductions up to 35%. The behavior obtained with 0 MW grid receptiveness fully corresponds also to the behavior that would be obtained if the return to the grid is allowed, but not paid by the grid, which is the actual current situation in Croatia.

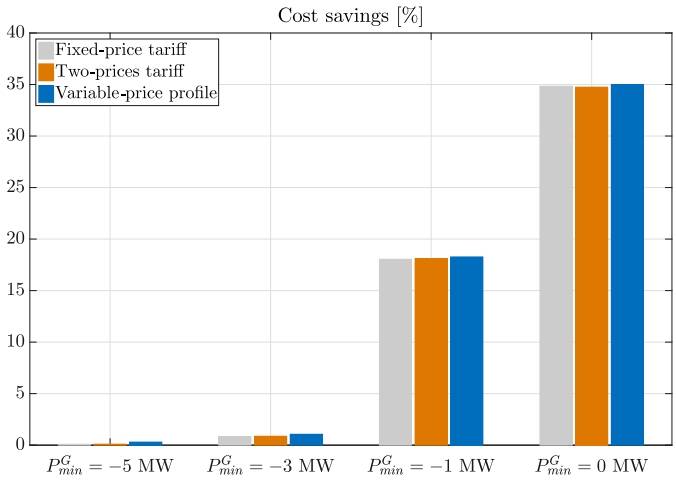

Fig. 8: Cost savings for one-day system operation for different grid receptiveness $P^{\mathrm{G}}_{\mathrm{min}}$, with only HHL MPC installed.

C. Coordination between levels

After the introduction of both the LHL and HHL control systems, it is possible to hierarchically coordinate them with the main goal of further increasing the energy efficiency and decreasing the system operation costs.

The hierarchical coordination algorithm is simulated for the period between 13:00 and 14:00 hours with all together 13 trains supplied from ETS Andrijevci at some point during the one-hour period, according to the timetable. Due to the hourly energy exchange price, there are no price changes during the considered period, and the grid receptiveness level is set to 0 MW i.e. no energy can be returned to the grid. Scenario with no energy returned to the grid directly corresponds to the case found in Croatia where the energy returned to the grid is not reimbursed. The simulated system operation is depicted with (i) energy storage power flows (battery and supercapacitor charging/discharging) together with energy dissipated on the resistors, (ii) ETS power flows (summed energy consumption/production of all trains currently supplied from ETS Andrijevci) and (iii) energy storage SoC, all

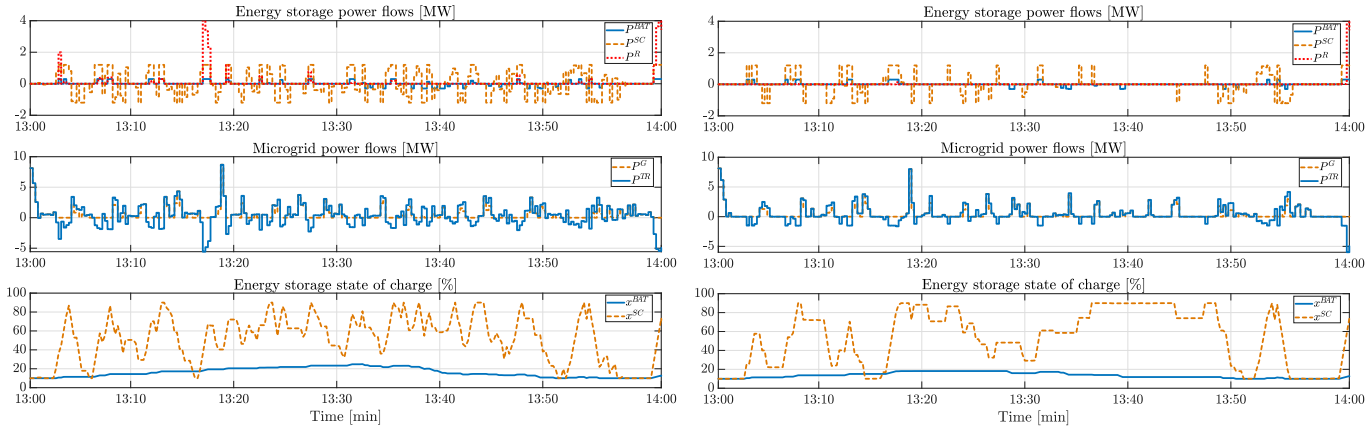

(a) Without coordination where only LHL solution θ^{h} is plugged into HHL problem (17).

(b) With hierarchical coordination between LHL and HHL employed.

Fig. 9: Comparison of one-hour system behavior with and without hierarchical coordination employed.

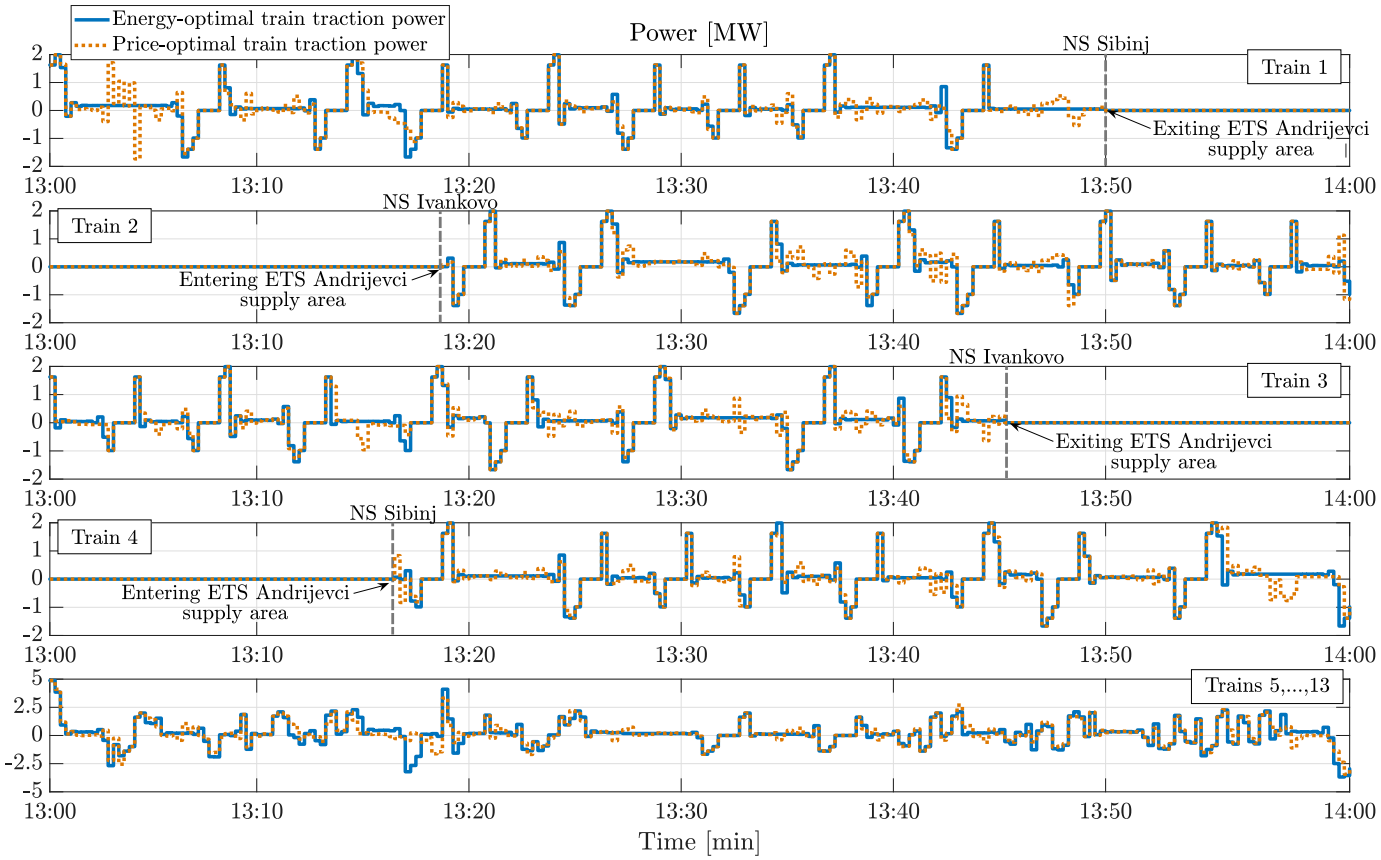

Fig. 10: Power consumption profiles of all trains supplied from ETS Andrijevci, before and after hierarchical coordination, for a one-hour system operation.

presented in Fig. 9 for the system operation before and after hierarchical coordination is employed.

From the results presented in Fig. 9, the following is observed: (i) the coordination between the control levels reduces the amount of energy that is being unused (dissipated in the resistors) through simultaneous coordination of different trains and their acceleration and deceleration while respecting the previously set timetable constraints (presented with red line in first plots of both a) and b) figures), (ii) the peaks of produced regenerative energy are reduced as the regenerative energy production from a single train is being distributed towards other trains that are able to accelerate during that period (presented with blue lines in middle plots of both a) and b) figures) and (iii) it is also observed that the use of the energy storage systems is reduced since their operation causes energy losses due to energy efficiency of the storage

technologies (presented in red and orange lines in first and last plots of a) and b) figures). Reduced energy storage usage brings additional benefits in terms of storage system health preservation and extended equipment lifetime.

Power consumption of individual trains during this one-hour simulation period is presented in Fig. 10, individually for four trains that are supplied during the most of the one-hour period, and cumulatively for the remaining 9 trains. Previously mentioned assumptions are confirmed, the neighboring trains exchange energy and cooperate in order to reduce system operation costs. Such energy exchange between trains can be seen when more trains are in braking and therefore generate a large amount of energy that is then consumed by other trains currently supplied from the same ETS, which are now deviating from their initial traction profiles in order to consume that energy. Although these trains then operate with a suboptimal traction profile and actually consume more energy, the system benefits from this interaction between trains since most of the regenerative braking energy would be dissipated if the trains would not be coordinated. This behavior can be seen in Fig. 10 where e.g. Train 1 speeds up at 13:03 to consume the energy generated by the remaining trains and reduce the cumulative regenerative energy peak (subplot 5), or where trains 3 and 4 brake early at 13:15 and 13:17, respectively, to shift their consumptions profile and reduce the overall regenerative energy production from 13:17-13:18 (subplot 5). Although the trains initial traction profiles are changed when the trains take into account the declared price profile, state of energy storages and various power grid requests, the schedule remains unchanged and operational constraints are respected.

In order to fully investigate the contributions and savings possibilities of hierarchical coordination between energy flows and consumption levels, different variations are introduced to the initial simulation set-up, with corresponding cost and energy consumption reductions compared and results presented in Fig. 11. Cost and energy reduction quantities in all cases are obtained through comparison with the costs and energy consumption of system operation without the HHL control and with trains driven in energy-optimal ways. Results obtained via solely MPC applied to higher level control with energy-optimal traction profiles applied for individual trains, but without coordination are then compared with the baseline case and compared to the results achieved with coordination in order to investigate what the coordination brings in terms of cost and energy efficiency. Presented results show that the energy consumptions reductions reach up to 40% while the costs are reduced up to 45%, as presented in Fig. 11.

An additional simulation case has been added to the setup, in order to investigate system operation without energy storage systems implemented and with coordination between the levels. From the results presented in Fig. 11 it is observed that software-based coordination on the lower level can eliminate the need for storages, since the cost reductions are only slightly decreased when no energy storage systems are installed in the system. Although such control system setup does not provide the best possible results, it also does not require large financial investments for installation of energy storage systems. It is therefore more close to implementation on actual railway systems and shows an important advantage of the analyzed hierarchical coordination.

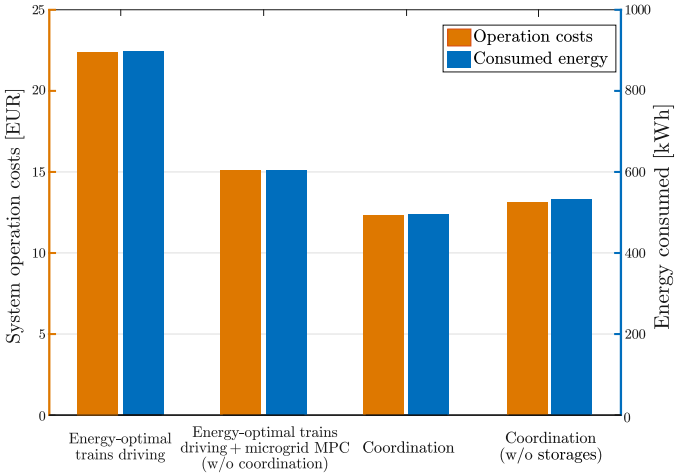

Fig. 11: Energy consumption and system operation costs for different control setups for the one-hour system operation.

VI. Conclusion

In this paper, an algorithm for energy- and cost-efficient control of the electric railway system is presented. The algorithm is based on hierarchical coordination of the electric traction substation energy flows control level (higher) and individual trains traction energy consumption control level (lower). On the lower level, individual consumption cost of energy used for trains traction is minimized while taking into account route and timetable constraints. On the higher control level, energy flows of a single electric traction supply substation, comprised of trains energy production/consumption and stationary energy storages, are optimized with respect to the cost for energy exchanged with the power grid.

The algorithm is verified on a detailed case study with an actual rail route and trains of an existing commercial brand traveling along it. The presented results show promising savings possibilities, which reach up to 45% cost reduction and 40% reduction of energy consumed. Each level of the presented modular control system contributes to savings increase, while keeping the possible implementations of the control system flexible and adaptable to various railway system configurations. Through interaction with the power grid, the railway system is transformed from a passive energy consumer into a proactive system capable of responding to various grid demands as well as provide services to the power grid operator.

Acknowledgment

The authors would like to thank Končar - Electric Vehicles Inc. for provided electromotive train data and Croatian Railways Infrastructure (HŽ Infrastruktura) for provided Section X rail track data and the corresponding timetables. This research has been carried out within the activities of the Centre of Research Excellence for Data Science and Cooperative Systems supported by the Ministry of Science and Education of the Republic of Croatia.

REFERENCES

[1] International Energy Agency and International Union of Railways, "Railway Handbook 2017 - Energy Consumption and CO_2 Emissions."

[2] European Commission, "A policy framework for climate and energy in the period from 2020 to 2030."

[3] I. M. Golovitcher, "Energy efficient control of rail vehicles," in *2001 IEEE International Conference on Systems, Man and Cybernetics. e-Systems and e-Man for Cybernetics in Cyberspace (Cat.No.01CH37236)*, vol. 1, 2001, pp. 658–663 vol.1.

[4] P. Howlett, "The optimal control of a train," *Annals of Operations Research*, vol. 98, no. 1, pp. 65–87, 2000.

[5] Y. Wang, B. Ning, F. Cao, B. De Schutter, and T. van den Boom, "A survey on optimal trajectory planning for train operations," in *Proceedings of 2011 IEEE International Conference on Service Operations, Logistics and Informatics*, 2011, pp. 589–594.

[6] S. Lu, S. Hillmansen, T. K. Ho, and C. Roberts, "Single-train trajectory optimization," *IEEE Transactions on Intelligent Transportation Systems*, vol. 14, no. 2, pp. 743–750, 2013.

[7] Y. Bai, T. K. Ho, B. Mao, Y. Ding, and S. Chen, "Energy-efficient locomotive operation for Chinese mainline railways by fuzzy predictive control," *IEEE Transactions on Intelligent Transportation Systems*, vol. 15, no. 3, pp. 938–948, 2014.

[8] J. Huang, Y. Deng, Q. Yang, and J. Sun, "An energy-efficient train control framework for smart railway transportation," *IEEE Transactions on Computers*, vol. 65, no. 5, pp. 1407–1417, 2016.

[9] Y. Wang, B. Ning, F. Cao, and T. van den Boom, and B. De Schutter, *Optimal Trajectory Planning and Train Scheduling for Urban Rail Transit Systems*. Springer International Publishing, 2016.

[10] Z. Li, L. Chen, C. Roberts, and N. Zhao, "Dynamic trajectory optimization design for railway driver advisory system," *IEEE Intelligent Transportation Systems Magazine*, vol. 10, no. 1, pp. 121–132, 2018.

[11] H. Dong, H. Zhu, and S. Gao, "An approach for energy-efficient and punctual train operation via driver advisory system," *IEEE Intelligent Transportation Systems Magazine*, vol. 10, no. 3, pp. 57–67, 2018.

[12] X. Yang, X. Li, Z. Gao, H. Wang, and T. Tang, "A cooperative scheduling model for timetable optimization in subway systems," *IEEE Transactions on Intelligent Transportation Systems*, vol. 14, no. 1, pp. 438–447, 2013.

[13] A. Nasri, M. F. Moghadam, and H. Mokhtari, "Timetable optimization for maximum usage of regenerative energy of braking in electrical railway systems," in *SPEEDAM 2010*, 2010, pp. 1218–1221.

[14] X. Yang, A. Chen, X. Li, B. Ning, and T. Tang, "An energy-efficient scheduling approach to improve the utilization of regenerative energy for metro systems," *Transportation Research Part C: Emerging Technologies*, vol. 57, pp. 13 – 29, 2015.

[15] Y. Jiang, J. Liu, W. Tian, M. Shahidehpour, and M. Krishnamurthy, "Energy harvesting for the electrification of railway stations: Getting a charge from the regenerative braking of trains," *IEEE Electrification Magazine*, vol. 2, no. 3, pp. 39–48, 2014.

[16] F. Ciccarelli, A. D. Pizzo, and D. Iannuzzi, "Improvement of energy efficiency in light railway vehicles based on power management control of wayside lithium-ion capacitor storage," *IEEE Transactions on Power Electronics*, vol. 29, no. 1, pp. 275–286, 2014.

[17] T. Ratniyomchai, S. Hillmansen, and P. Tricoli, "Recent developments and applications of energy storage devices in electrified railways," *IET Electrical Systems in Transportation*, vol. 4, no. 1, pp. 9–20, 2014.

[18] S. de la Torre, A. Sanchez-Racero, J. Aguado, M. Reyes, and O. Martianez, "Optimal sizing of energy storage for regenerative braking in electric railway systems," *IEEE Transactions on Power Systems*, vol. 30, no. 3, pp. 1492–1500, 2015.

[19] P. Arboleya, P. Bidaguren, and U. Armendariz, "Energy is on board: Energy storage and other alternatives in modern light railways," *IEEE Electrification Magazine*, vol. 4, no. 3, pp. 30–41, 2016.

[20] F. Zhu, Z. Yang, H. Xia, and F. Lin, "Hierarchical control and full-range dynamic performance optimization of the supercapacitor energy storage system in urban railway," *IEEE Transactions on Industrial Electronics*, vol. 65, no. 8, pp. 6646–6656, 2018.

[21] A. Clerici, E. Tironi, and F. Castelli-Dezza, "Multiport converters and ess on 3-kv dc railway lines: Case study for braking energy savings," *IEEE Transactions on Industry Applications*, vol. 54, no. 3, pp. 2740–2750, 2018.

[22] X. Yang, X. Li, B. Ning, and T. Tang, "A survey on energy-efficient train operation for urban rail transit," *IEEE Transactions on Intelligent Transportation Systems*, vol. 17, no. 1, pp. 2–13, 2016.

[23] S. Su, T. Tang, X. Li, and Z. Gao, "Optimization of multitrain operations in a subway system," *IEEE Transactions on Intelligent Transportation Systems*, vol. 15, no. 2, pp. 673–684, 2014.

[24] S. Su, T. Tang, and C. Roberts, "A cooperative train control model for energy saving," *IEEE Transactions on Intelligent Transportation Systems*, vol. 16, no. 2, pp. 622–631, 2015.

[25] X. Yang, X. Li, B. Ning, and T. Tang, "An optimisation method for train scheduling with minimum energy consumption and travel time in metro rail systems," *Transportmetrica B: Transport Dynamics*, vol. 3, no. 2, pp. 79–98, 2015.

[26] X. Sun, H. Lu, and H. Dong, "Energy-efficient train control by multi-train dynamic cooperation," *IEEE Transactions on Intelligent Transportation Systems*, vol. 18, no. 11, pp. 3114–3121, 2017.

[27] E. Pilo de la Fuente, S. Mazumder, and I. Gonzalez Franco, "Railway electrical smart grids: An introduction to next-generation railway power systems and their operation." *IEEE Electrification Magazine*, vol. 2, no. 3, pp. 49–55, 2014.

[28] P. Pankovits, J. Pouget, B. Robyns, F. Delhaye, and S. Brisset, "Towards railway-smartgrid: Energy management optimization for hybrid railway power substations," in *Innovative Smart Grid Technologies Conference Europe (ISGT-Europe), 2014 IEEE PES*, 2014.

[29] J. A. Aguado, A. J. S. Racero, and S. de la Torre, "Optimal operation of electric railways with renewable energy and electric storage systems," *IEEE Transactions on Smart Grid*, vol. 9, no. 2, pp. 993–1001, 2018.

[30] I. Sengor, H. C. Kilickiran, H. Akdemir, B. Kekezoglu, O. Erdinc, and J. P. S. Catalao, "Energy management of a smart railway station considering regenerative braking and stochastic behaviour of ess and pv generation," *IEEE Transactions on Sustainable Energy*, vol. 9, no. 3, pp. 1041–1050, 2018.

[31] S. Khayyam, F. Ponci, J. Goikoetxea, V. Recagno, V. Bagliano, and A. Monti, "Railway energy management system: Centralized-decentralized automation architecture," *IEEE Transactions on Smart Grid*, vol. 7, no. 2, pp. 1164–1175, 2016.

[32] H. Novak, M. Vašak, and V. Lešić, "Railway transport system energy flow optimization with integrated microgrid," in *Proceedings of the 12th International Conference on Modern Electrified Transport, MET 2015*, 2015, pp. 88–94.

[33] M. Vašak, M. Baotić, N. Perić, and M. Bago, "Optimal rail route energy management under constraints and fixed arrival time," in *Proceedings of the European Control Conference 2009*, 2009, pp. 2972–2977.

[34] H. Novak, M. Vašak, and V. Lešić, "Hierarchical energy management of multi-train railway transport system with energy storages," in *2016 IEEE International Conference on Intelligent Rail Transportation (ICIRT)*, 2016, pp. 130–138.

[35] H. Novak, V. Lešić, and M. Vašak, "Hierarchical coordination of trains and traction substation storages for energy cost optimization," in *2017 IEEE 20th International Conference on Intelligent Transportation Systems (ITSC)*, 2017, pp. 1–6.

[36] H. Novak and M. Vašak, "Energy-efficient train traction control on complex rail configurations," in *2018 26th Mediterranean Conference on Control and Automation (MED)*, 2018.

[37] M. Gulin, M. Vašak, and M. Baotić, "Analysis of microgrid power flow optimization with consideration of residual storages state," in *2015 European Control Conference (ECC)*, 2015, pp. 3126–3131.

[38] F. Borrelli, A. Bemporad, and M. Morari, "Geometric algorithm for multiparametric linear programming," *Journal of Optimization Theory and Applications*, vol. 118, no. 3, pp. 515–540, 2003.

[39] HŽ Infrastruktura Ltd., "Network Statement 2015," 2014.

[40] Končar Electric Vehicles Inc., "Electric Multiple Units," http://www.koncar-kev.hr/products_and_services/electric_multiple_units.

[41] Končar Electric Vehicles Inc., "Low-floor Electric Multiple Unit for Urban and Commuter Operation," http://www.koncar-kev.hr/docs/koncarkevEN/documents/19/2_1/Original.pdf.

[42] "EPEX SPOT. European Power Exchange Electricity Index." [Online]. Available: http://www.epexspot.com

[43] "Maxwell Technologies Inc. - Ultracapacitors overview." [Online]. Available: http://www.maxwell.com/products/ultracapacitors/

[44] "Saft Batteries - Intensium Max for efficient trackside energy storage." [Online]. Available: https://www.saftbatteries.com/products-solutions/products/intensium-max-efficient-trackside-energy-storage

Hrvoje Novak (S'12-M'17) received his M.Sc.E.E. degree from University of Zagreb Faculty of Electrical Engineering and Computing, Croatia in 2014. Currently, he is a research assistant at the Department of Control and Computer Engineering and a member of the Laboratory for Renewable Energy Systems. His research interests are in the domain of advanced control algorithms with application to railway transport systems and neural network based prediction algorithms in building systems. He authored and co-authored several scientific and professional papers in the field of railway system energy efficiency, model predictive control and hierarchical coordination of railway transport subsystems.

Vinko Lešić (S'09-M'15-SM'17) received his PhD degree in 2014 from University of Zagreb Faculty of Electrical Engineering and Computing, Zagreb, Croatia (UNIZG-FER). Currently, he is an assistant professor at the Department of Control and Computer Engineering of UNIZG-FER. His focus is on control theory and its application to renewable energy systems and smart city technologies or more particularly, model predictive control for buildings and transport energy efficiency and microgrid operation. He co-authored more than 30 journal and conference papers and a patent. He is an active volunteer of IEEE Region 8.

Mario Vašak (M'07) is a full professor at the Department of Control and Computer Engineering, University of Zagreb Faculty of Electrical Engineering and Computing and he is heading its Laboratory for Renewable Energy Systems. His research interests are in the domain of dynamic systems predictive control with applications to systems from the low-carbon energy sector. He is the main inventor of the US patent for fault-tolerant control of wind turbine generators and has designed the concept of hierarchical and modular energy management in buildings with integrated microgrids for enabling their economically optimal interoperation. He authored more than 15 papers in international scientific journals and overall more than 100 internationally reviewed papers. He served as president of Control Systems Chapter of the IEEE Croatia Section in period 2014-2017.